

# Vehicle Heading Angle Determination Using Magnetometer

Seon-Ho Lee\* and Hyo-Sung Ahn\*\*

\* Satellite Control System Dept., Korea Aerospace Research Institute, Taejon, Korea.  
(Tel : +82-42-860-2035; E-mail: shlee71@kari.re.kr)

\*\* Department of Electrical Engineering, University of North Dakota, Grand Forks, ND, USA.  
(Tel : +1-701-777-2553; E-mail: hyo.ahn@und.edu)

**Abstract:** The vehicle's heading angle determination is formulated and the proposed method based on geometry engages the magnetometer and the GPS. The resulting maximum determination accuracy of 0.3deg over the entire earth as a standard deviation is obtained for a magnetometer with measurement error of 1nT.

**Keywords:** Heading Angle Determination, Magnetometer, GPS, IGRF

## 1. Introduction

The current state of the vehicle determination and compass application using with the earth's field range was described using magnetometer in various articles[1-2]. Usually the compassing algorithm is formulated with measured earth's magnetic field that was approximated by a dipole field. In this case, the variation angle should be compensated with an appropriate variation map over the entire earth. In other cases, the gyro-engaged Kalman filter are introduced to achieve more precision determination. The method introduced here uses a new alternative scheme with magnetometer without any variation compensation. The proposed method has several features. First, it doesn't require the gyro-based Kalman filter algorithm. Second, the determination algorithm based on the geometry has a conceptually simple structure but an effective method to determine the vehicle's heading angle. Third, the vehicle's roll and pitch angle information from the implemented gimbal system can be combined to obtain precision determination. The proposed algorithm is applicable to the vehicle navigation for heading angle determination and it can be used as a backup plan for the yaw gyroscopic compassing of satellites in case of gyro failure. Moreover, the proposed algorithm can be used to calculate an initial condition for the Kalman Filter based determination method.

## 2. Main Results

Assume that the vehicle's location on the earth is obtained with the latitude ( $\phi$ ) and longitude ( $\lambda$ ) for the global positioning system as shown in Figure 1.

The local meridian vector at the vehicle's location toward the geographic north denoted by  $\vec{n}$ , is given by

$$\vec{n} = [-\cos(90 - \phi) \cos(\lambda), -\cos(90 - \phi) \sin(\lambda), \sin(90 - \phi)]^T \quad (1)$$

The vehicle's body axes are defined by three unit vectors,  $\vec{x}$ ,  $\vec{y}$ , and  $\vec{z}$  where  $\vec{x}$  is the moving velocity vector,  $\vec{y}$  is the left-side lateral vector, and  $\vec{z}$  is the normal vector on the local level plane. Then, the three body axes are given by

$$\vec{x} = [p_x, p_y, p_z]^T \quad (2)$$

$$\vec{y} = [q_x, q_y, q_z]^T \quad (3)$$

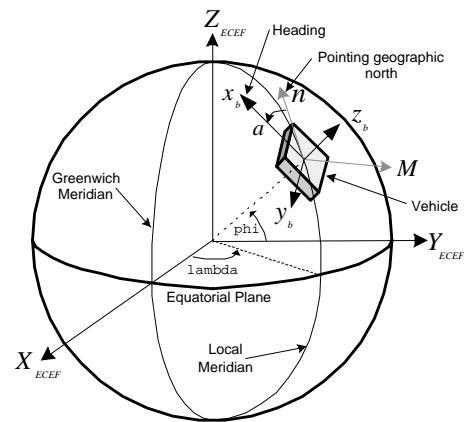


Fig. 1. Illustration of heading angle ( $a$ ) between vehicle's heading vector and geographic north pointing vector.

$$\vec{z} = [\cos(\phi) \cos(\lambda), \cos(\phi) \sin(\lambda), \sin(\phi)]^T \quad (4)$$

where the unknown components of  $(p_x, p_y, p_z)$  and  $(q_x, q_y, q_z)$  are variant depending on the heading angle and are to be determined. Since  $\vec{x}$  and  $\vec{y}$  are unit vectors, we obtain

$$\|\vec{x}\| = \|\vec{y}\| = 1 \quad (5)$$

Moreover, since both  $\vec{x}$  and  $\vec{y}$  are perpendicular to  $\vec{z}$  respectively, we obtain

$$\vec{x} \cdot \vec{z} = \vec{y} \cdot \vec{z} = 0 \quad (6)$$

The measured magnetic field vector denoted by  $B = [B_x, B_y, B_z]^T$ , is given by

$$B_x = M(\lambda, \phi) \cdot \vec{x} \quad (7)$$

$$B_y = M(\lambda, \phi) \cdot \vec{y} \quad (8)$$

where  $M = [M_x, M_y, M_z]^T$  is the reference earth's magnetic field model. From (5)-(8), we obtain

$$\begin{bmatrix} p_x & p_y & p_z \\ \cos(\phi) \cos(\lambda) & \cos(\phi) \sin(\lambda) & \sin(\phi) \\ M_x(\lambda, \phi) & M_y(\lambda, \phi) & M_z(\lambda, \phi) \end{bmatrix} \begin{bmatrix} p_x \\ p_y \\ p_z \end{bmatrix} = \begin{bmatrix} 1 \\ 0 \\ B_x \end{bmatrix} \quad (9)$$

$$\begin{bmatrix} q_x & q_y & q_z \\ \cos(\phi)\cos(\lambda) & \cos(\phi)\sin(\lambda) & \sin(\phi) \\ M_x(\lambda, \phi) & M_y(\lambda, \phi) & M_z(\lambda, \phi) \end{bmatrix} \begin{bmatrix} q_x \\ q_y \\ q_z \end{bmatrix} = \begin{bmatrix} 1 \\ 0 \\ B_y \end{bmatrix} \quad (10)$$

Solving (9) and (10) provides two possible solutions respectively such as  $\vec{x} \in \{\vec{x}_1, \vec{x}_2\}$  and  $\vec{y} \in \{\vec{y}_1, \vec{y}_2\}$ . In order to determine the exact solution, we define a cost function such as for  $i, j \in \{1, 2\}$

$$J_{ij} = \gamma \|\vec{x}_i \cdot \vec{y}_j\| + (1 - \gamma) \|\vec{x}_i \times \vec{y}_j - \vec{z}\| \quad (11)$$

where  $0 < \gamma < 1$ . Then, we select  $i = i^*$  and  $j = j^*$  that minimize  $J_{ij}$ . Finally, the heading angle along  $\vec{z}$  axis is determined as

$$\alpha = \text{sign}\{(\vec{x}_{i^*} \times \vec{n}) \cdot \vec{z}\} \cos^{-1}(\vec{x}_{i^*} \cdot \vec{n}) \quad (12)$$

The flow diagram of the proposed heading angle determination algorithm is described in Figure 2. We note that if  $M$  is parallel to  $z_b$ , then  $B_x$  and  $B_z$  approaches to zero, which means that the equations have infinite solutions.

Remark 1: If there exists a gimbal system on the vehicle to measure the roll and pitch tilt angle, more accurate determination is expected. In this case, in (9) and (10)  $B_x, B_y, B_z$  should be replaced with  $\bar{B}_x, \bar{B}_y, \bar{B}_z$  such as

$$\begin{bmatrix} \bar{B}_x \\ \bar{B}_y \\ \bar{B}_z \end{bmatrix} = \begin{bmatrix} 1 & 0 & 0 \\ 0 & \cos(\theta_r) & \sin(\theta_r) \\ 0 & -\sin(\theta_r) & \cos(\theta_r) \end{bmatrix} \begin{bmatrix} \cos(\theta_p) & 0 & \sin(\theta_p) \\ 0 & 1 & 0 \\ \sin(\theta_p) & 0 & \cos(\theta_p) \end{bmatrix} \begin{bmatrix} B_x \\ B_y \\ B_z \end{bmatrix} \quad (13)$$

where  $\theta_r$  and  $\theta_p$  are tilt angles obtained by the gimbal system.

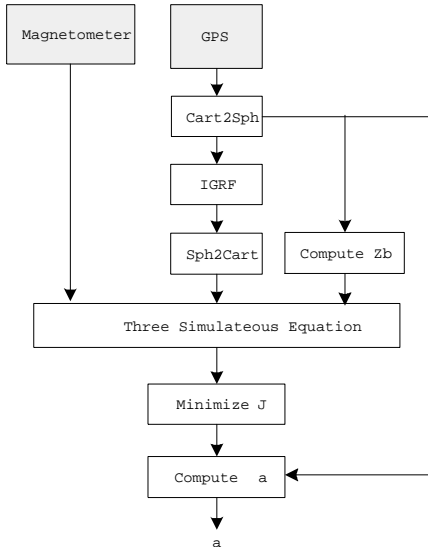


Fig. 2. Flow diagram of heading angle determination algorithm.

### 3. Simulation Results

The simulation is performed at the location of Taejon, Korea ( $\lambda = 127.4\text{deg}$  and  $\phi = 36.3\text{deg}$ ). The standard deviation ( $\sigma$ ) of determination accuracy is summarized in Table 1 for five cases of the introduced noise( $3\sigma$ ) at magnetometer.

Table 1. Standard deviation of determination accuracy at Taejon, Korea

Noise( $3\sigma$ )	Standard Deviation
0.01 nT	0.00037 deg
0.1 nT	0.0022 deg
1 nT	0.0098 deg
10 nT	0.061 deg
100 nT	0.33 deg

The simulation is performed over the entire earth. Table 2 summarizes maximum (worst case) standard deviation of determination accuracy. Figure 4-8 shows the standard deviation over the entire earth. We observe that the determination error increases as the vehicle approaches around the magnetic north and south poles.

Table 2. Standard deviation of determination accuracy over the entire earth.

Noise( $3\sigma$ )	Standard Deviation
0.01 nT	0.011 deg
0.1 nT	0.058 deg
1 nT	0.29 deg
10 nT	1.6 deg
100 nT	9.2 deg

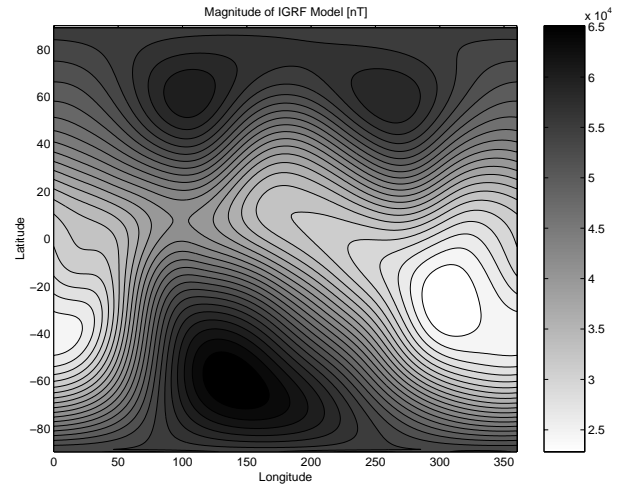


Fig. 3. Magnitude of geomagnetic field from IGRF model.

### 4. Conclusions

The vehicle's heading angle determination method is formulated using magnetometer and we demonstrate the performance of the proposed heading angle determination. The resulting maximum determination accuracy of less than 0.3deg over the entire earth for a magnetometer with measurement

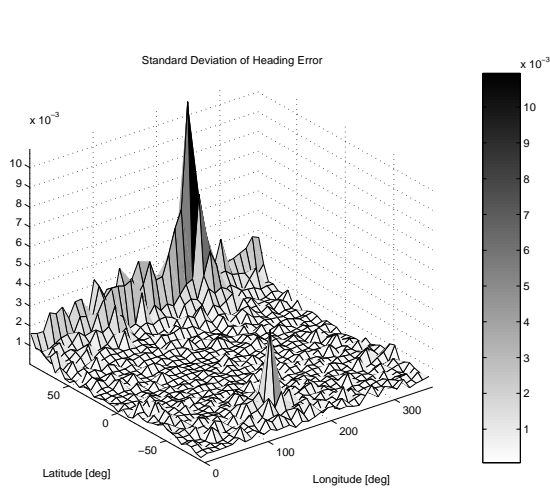


Fig. 4. Standard deviation of determination error over the entire earth for noise 0.01nT ( $3\sigma$ ).

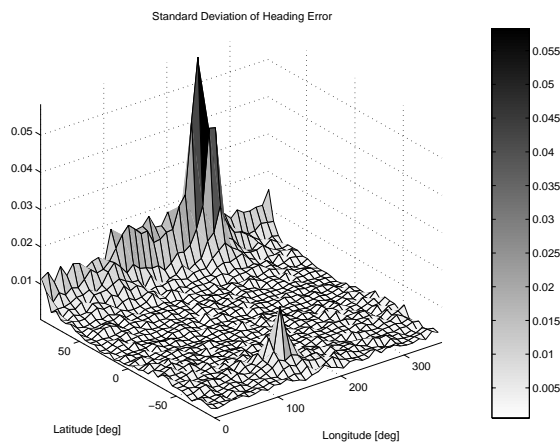


Fig. 5. Standard deviation of determination error over the entire earth for noise 0.1nT ( $3\sigma$ ).

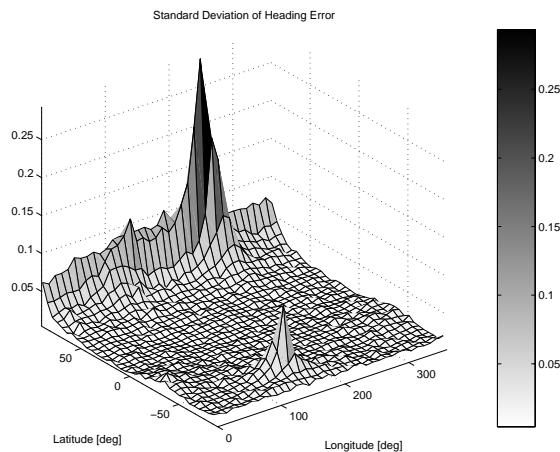


Fig. 6. Standard deviation of determination error over the entire earth for noise 1nT ( $3\sigma$ ).

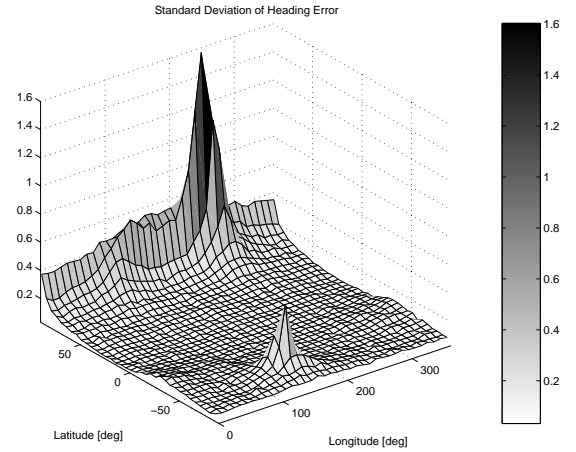


Fig. 7. Standard deviation of determination error over the entire earth for noise 10nT ( $3\sigma$ ).

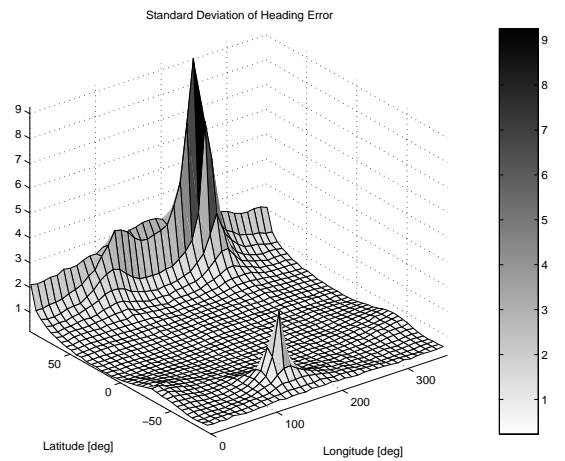


Fig. 8. Standard deviation of determination error over the entire earth for noise 100nT ( $3\sigma$ ).

accuracy of 1nT. The proposed method is efficiently used for the gyro-failure case.

## References

- [1] M.J. Caruso and L.S. Withanawasam, "Vehicle detection and compass applications using AMR magnetic sensors," Honeywell SSEC, Technical Articles, <<http://www.ssec.honeywell.com>>
- [2] R.B. Dyott, "Method for finding true north using a fibre-optic gyroscope," *Electronics Letters*, 1994, 30, (13), pp. 1087-1088.